

Superficial tissue optical property determination using spatially resolved measurements close to the source: Comparison with Frequency Domain Photon Migration measurements

Frédéric Bevilacqua^a, Dominique Piguet^a, Pierre Marquet^a, Jeffrey D. Gross^b, Dorota Jakubowski^b, Vasan Venugopalan^b, Bruce J. Tromberg^b and Christian Depeursinge^a

^aInstitute of Applied Optics,
Microengineering Department,
Swiss Federal Institute of Technology at Lausanne, Switzerland

^bLaser Microbeam and Medical Program,
Beckman Laser Institute and Medical Clinic,
University of California at Irvine, USA

ABSTRACT

Local and superficial optical property characterization of biological tissues can be performed by measuring spatially-resolved diffuse reflectance at small source-detector separations. Monte Carlo simulations and experiments were performed to assess the performance of a spatially-resolved reflectance probe, employing multiple detector fibers (0.3 to 1.4 mm from the source). Under these conditions, the inverse problem, i.e. calculating the absorption and reduced scattering coefficients, is necessarily sensitive to the phase function. This effect must be taken into account by considering a new parameter of the phase function, which depends on the first and second moments of the phase function. Probe performance is compared to another technique for quantitatively measuring optical coefficients, based on the analysis of photon density waves (Frequency Domain Photon Migration). The two techniques are found to be in reasonable agreement. However, the spatially resolved probe shows optimum measurement sensitivity in the volume immediately beneath the probe, while FDPM typically samples much larger regions of tissues. Measurements on human brain *in vivo* are reported using both methods.

Keywords: Turbid Media, Photon migration, Optical diagnostics for medicine, Optical biopsy, Neural tissues.

1. INTRODUCTION

Light propagation in biological tissue is highly sensitive to the structure and biochemical composition of critical components such as cells and sub-cellular components, the surrounding matrix, blood vessels and flow. Consequently, optical tools can provide physicians with diagnostic information that is uniquely sensitive to physiology. We focus here on the *in vivo* measurement of absorption and elastic scattering properties. These properties can provide information both on tissue structure and chromophore content, features which can be used to distinguish between normal tissues, malignant lesions and other pathologies. For example hemoglobin and water content have been found to be significantly different in normal and cancerous tissues^{1,2}. Differentiation between normal and malignant bladder tissues³ was found to be possible from the elastic scattering and absorption properties.

The measurement of the tissue optical properties can also impact other biomedical applications. For example, the knowledge of these properties is necessary for optimizing techniques such as oximetry, near-infrared spectroscopy and photodynamic therapy. The scattering and absorption characteristics of many different kinds of tissues have been reported in the literature⁴. However, they have been mostly measured *in vitro*. Because of unavoidable alterations of excised samples, such as blood drainage, structural alterations, temperature and hydration changes, these values are questionable and *in vivo* measurements are preferable.

Several methods have already been proposed to quantitatively determine the absorption and reduced scattering coefficients *in vivo*, using spatially⁵⁻⁷ and/or temporally-resolved reflectance measurements^{1,2,8}. To our knowledge, the separate

Correspondance: frederic.bevilacqua@epfl.ch,
see Microvision and Microdiagnostic in <http://dmtwww.epfl.ch/ioa/research.html>

determination of the absorption and scattering parameters have been so far performed *in vivo* on biological tissues using large source-detector separations (typically from 2 to 15 mm). Therefore, the volume probed is on the order of 1 cm³, and relatively large tissue parts are characterized by an average value which can be difficult to interpret. For optical biopsy purposes, it is important to probe a smaller part of tissue. For this reason, we developed a probe using only small source-detector separations (<1.5 mm). The volume probed is significantly smaller (on the order of 1 mm³). Moreover, such a thin probe can be put in endoscopes or can be used during minimally-invasive surgery.

Other groups have proposed small diameter probes for *in vivo* investigation. For example, Reynolds et al⁹ and Ono et al¹⁰ have shown that blood oxygenation can be monitored with small probes ($\varnothing < 2$ mm). Mourant and coworkers^{3,11} have also shown that the backscattered light, measured at a single shorter distance (approximately 0.3-0.4 mm), can provide spectroscopic signatures between normal and malignant tissues. They have also shown that the tissue absorption coefficient can be estimated with a measurement at a single distance of approximately 1.7 mm, assuming the scattering coefficient to be in a certain range. However, none of these approaches allows for the simultaneous determination of unknown absorption and reduced scattering coefficients.

In this work, we address a general case where both tissue scattering and absorption properties are simultaneously determined, using a small diameter probe ($\varnothing=2$ mm). The method is based the measurement of the spatially-resolved reflectance, at small source-detectors separations (0.3-1.4 mm). A theoretical model, based on Monte Carlo simulations was developed to determine the absorption and scattering parameters from the reflectance curve.

We believe that the estimation of both absorption and scattering coefficients is crucial to correlate the optical data with the tissue physiology. Indeed, the absorption spectra can provide the local concentration of components such as oxy- and deoxy-hemoglobin and water. The scattering spectra may provide information about the size and density of cells and organelles. The access to such quantities should importantly increase the specificity of the diagnosis and facilitates the medical interpretation of optical measurements.

In this paper, we first describe the probe design and the theoretical model that we developed to determine the absorption and scattering parameters from the measurement. Second, we present clinical results performed on human brain *in vivo* during surgery. These clinical measurements were performed in parallel with a complementary method, frequency domain photon migration (FDPM)^{2,3}, which probes a larger tissue volume (source-detector separation larger than 10 mm). Optical properties from FDPM measurements are compared with values obtained using the spatially-resolved method described here, using small source-detector separations.

2. MATERIAL AND METHOD

2.1. Definitions

The spatially resolved reflectance is denoted $R(\rho)$ where ρ is the source-detector separation. It is defined by the backscattered power received by a detector per unit area for a source of power unity. In our measurements, ρ ranges between 0.3 and 1.4 mm.

The optical properties of tissues are the average refractive index n of the medium, the absorption coefficient μ_a , the scattering coefficient μ_s , and the phase function $p(\theta)$ where θ is the scattering angle. The phase function is the probability density function for θ . We consider the refractive index of tissues¹² as a constant $n=1.4$.

The phase function can be parameterized by its Legendre moments, defined as follows:

$$g_n = 2\pi \int_0^\pi P_n(\theta) p(\theta) \sin(\theta) d\theta \quad (1)$$

where $P_n(\theta)$ is the Legendre function of order n .

The zero-order moment g_0 is normalized to 1 for any phase function. The first-order moment g_1 represents the mean cosine of the scattering angle θ . g_1 is also often called the anisotropy factor (or asymmetry factor), and it is usually simply noted g in tissue optics. Thus, please note that $g_1=g$.

It is also useful to define the reduced scattering coefficient $\mu_s' = \mu_s(1-g_1)$ and the transport mean free path $mfp' = (\mu_s' + \mu_a)^{-1}$. Generally the reduced scattering coefficient μ_s' and the absorption coefficient μ_a are used to characterize optically thick tissue. Indeed, for a high albedo medium, the light fluence rate depends only on μ_s' and μ_a at distances of several transport mean free paths (typically $\rho > 5$ mm for tissues) from the source (diffusion approximation). Therefore the use of μ_s' and μ_a is a natural choice if measurements are performed at such distances. As we want to make measurements at closer distances, in the range of one transport mean free path, we expect that several moments of the phase function must be taken into account. This theoretical problem was fully studied with Monte Carlo simulations¹³, and the main implications of this work are reported in the results section.

2.2. Similarity relations

Wyman et al.¹⁴ derived interesting similarity relations which we found useful for the description of $R(\rho)$, close to the source. These relations expressed how a set of optical parameters $\mu_a, \mu_s, g_1, g_2, \dots$ can be transformed into a second set $\mu_a^*, \mu_s^*, g_1^*, g_2^*, \dots$, without causing variation of the reflectance $R(\rho)$, at least for a restricted range of distances. Therefore, the similarity relations allow for the reduction of relevant parameters necessary to describe $R(\rho)$.

As will be shown in the results section, we found that the so-called second order similarity relation¹⁴ can be applied for $R(\rho)$ close to the source:

$$\begin{aligned} \mu_a &= \mu_a^* & (2) \\ \mu_s(1-g_1) &= \mu_s^*(1-g_1^*) \Rightarrow \mu_s' = \mu_s'^* & (3) \\ \mu_s(1-g_2) &= \mu_s^*(1-g_2^*) & (4) \end{aligned}$$

The second order similarity relations (Eqs 2,3,4) are valid when the radiance is 2nd order anisotropic (or “quadratically anisotropic”), i.e. it can be expanded in Legendre functions of the first and second order (see Ref.14). Thus this is a less restrictive approximation than the diffusion approximation (linear anisotropic radiance). To clarify the interpretation of the third relation (Eq.4), we introduce a new phase function parameter γ defined as follows:

$$\gamma = (1-g_2)/(1-g_1) \quad (5)$$

Therefore, Eq.3 and Eq.4 can be rewrite as follows:

$$\begin{aligned} \mu_s(1-g_1) &= \mu_s^*(1-g_1^*) \Rightarrow \mu_s' = \mu_s'^* & (6) \\ (1-g_2)/(1-g_1) &= (1-g_2^*)/(1-g_1^*) \Rightarrow \gamma = \gamma^* & (7) \end{aligned}$$

We see that these second order similarity relation imply that only one additional phase function parameter γ must be considered, compared to the case of the diffusion approximation. It is crucial to note that this parameter is not g_1 ($=g$), but a parameter which takes into account the first and second moments of the phase function.

2.3. Monte Carlo Simulations

A model of photon migration in tissues is necessary to define the relationship between the measured reflectance and the optical properties. Analytical solutions from the diffusion equation are not appropriate in our case because we are interested in the reflectance close to the source, at a distance comparable to the transport mean free path [mfp']^{5,13}. We performed Monte Carlo simulations to predict the measured reflectance of an homogeneous semi-infinite turbid media. The code we used was extensively tested^{13,15,16}. Any phase function can be implemented in discretized form.

Our simulations take into account the exact diameter of the illuminating and collecting fibers, as well as their numerical apertures (NA=0.28 in tissue). The mismatch of index of refraction at the surface of the medium is also taken into account in our simulation, by using the Fresnel law for each photon reaching the surface.

2.4. Experimental setup

2.4.1. Spatially-resolved probe measurement

The probe used for the measurement of the spatially resolved reflectance is described in Fig.1. It is a linear array of optical fibers (core diameter of 200 μm , N.A. = 0.37 in air). Two source fibers can be used to illuminate the tissue. They are positioned symmetrically with respect to the collecting fibers. If the sample is homogeneous, the reflectance curve is identical with either illuminating fiber. Therefore, comparing the two curves tests the heterogeneity of the investigated tissue region or detects obstructions, beneath the illuminating fibers. If the two curves are close (typically differences less than 10%), the measurement is validated and the average of the two curves is calculated.

The illuminating fibers are slid in small stainless steel tubes in order to avoid direct light coupling with the collecting fibers. The coupling between each collecting fiber has been experimentally measured and found to be less than 2%. The fiber array is set in a stainless steel tube of 2.5 mm diameter and 20 cm long. The tube is filled with an adhesive. The probe is rigid, which allows for easier handling by the physician, during surgery for example. The whole probe can be sterilized.

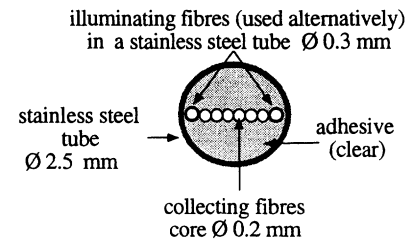


Fig.1 Optical probe

An optical switch (Dicon, model GP700) is used to select the illuminating fiber from different sources. Four laser diodes emitting at 674 nm, 811 nm, 849 nm and 956 nm were used (SDL, Inc. models 7421, 5420, 5421 and 6321, respectively). The six fibers used to collect the backscattered light are imaged on a linear Charge-Coupled-Device (CCD) (Hamamatsu S3921). The signal is digitized by a 12 bit A/D card. A simple measurement, which takes approximately 0.1 s, is then needed to measure simultaneously the intensity collected by the six fibers. The entire system is controlled by a personal computer.

Transmission differences between each fiber are corrected using a measurement on a turbid phantom illuminated uniformly. Immediately after each reflectance measurement, a measurement of the background light is automatically performed and then subtracted from the reflectance signal. To minimize the background light, a long pass filter ($\lambda > 650$ nm) is put between the end of the bundle and the CCD. Even during open surgery where the ambient light is substantial, the measured background was less than 5% of the signal.

In order to perform absolute intensity measurements, calibration is performed on a solid turbid siloxane phantom of known optical properties (determined independently by frequency domain photon migration^{2,3}).

2.4.2. Frequency Domain Photon Migration measurement (FDPM).

The optical coefficients μ_a and μ_s' can be determined from frequency domain reflectance measurements (referred to as FDPM for Frequency Domain Photon Migration). The instrument, developed at the Beckman Laser Institute and Medical Clinic, has been previously extensively described.^{1,2} It is based on the use of intensity-modulated laser diodes as sources and an avalanche photodiode as the detector. A network analyzer (Hewlett Packard model 8753C) measures the amplitude (A) and the phase shift of the backscattered light. (F). For all the measurements reported, we recorded 201 frequency points per sweep. Typically, acquisition time is 45 seconds when 5 frequency sweeps from 20 MHz to 1 GHz are taken at each of 4 wavelengths.

FDPM measurements are recordings of phase shift (F) and AC amplitude (A) at each modulation frequency. The values measured actually account for both the contribution of the turbid medium under investigation and the optical/electronic characteristics of the system, or what we simply refer to as the instrument response. To isolate the contribution of the sample, characterized by its phase shift F_{medium} and its AC amplitude A_{medium} , to the measured phase shift F_{meas} and amplitude attenuation A_{meas} , a calibration step must be performed. In summary, a measurement on a solid homogeneous phantom of known optical properties is performed at each wavelength before (or after) each measurement session. The instrument response is obtained by comparing measured F_{meas} and A_{meas} values with those expected for the calibration standard.

The phase shift F_{medium} and the AC amplitude A_{medium} is given by the solution of the diffusion equation. The solution for the semi-infinite space has been solved by Haskell et al.¹⁷ using the method of image. The optical coefficients μ_a and μ_s' are then obtained by a modified Levenberg-Marquardt algorithm¹⁸, fitting simultaneously the two quantities F_{medium} and A_{medium} .

3. RESULTS

3.1. Effect of the phase function

It is well known that the use of the diffusion approximation to predict optical transport is not valid proximal to a light source. In these locations, the diffuse reflectance depends not only on μ_a and μ_s' , but also on some parameters of the phase function. In particular, we studied the effect of the different moment g_n of the phase function on $R(\rho)$ with Monte Carlo simulations¹⁵. We found that both the first and second moment, $g_1 (=g)$ and g_2 must be taken into account for distances larger than $0.5 \text{ mfp}'$, whereas the effect are higher moments are comparatively weak.

We insist here that the second moment g_2 must be considered. Fig.2 shows different reflectance curves with constant $g_1 = 0.9$ but varying g_2 values: 0.75, 0.81, 0.9. It clearly demonstrates that the g_2 value can induce, for constant g_1 , differences in the reflectance up to 30% at distances $0.5 < \rho\mu_s' < 2$.

However, the effect of g_1 and g_2 on $R(\rho)$ is not independent. Indeed, the important parameter to consider is $\gamma = (1-g_2)/(1-g_1)$, which takes into account g_1 and g_2 (see section 2.2). To demonstrate the validity of this similarity relation, we report in Fig.3 the reflectance computed with three different phase functions characterized by identical $\gamma = 1.25$, but different g_1 and g_2 values ($g_1 = 0.2, 0.5, 0.9$ and $g_2 = 0, 0.375, 0.875$ respectively). Fig. 3 shows that these similarity relations are satisfied within only 2% error margin for optical distances $\rho\mu_s' > 0.5$, in the case $n = 1.0$. For the case $n=1.4$, slightly higher differences are found (<10%, for $\rho\mu_s' > 0.5$). Note that these differences are much lower than the ones found in Fig.2 where g_2 was varied, and g_1 kept constant.

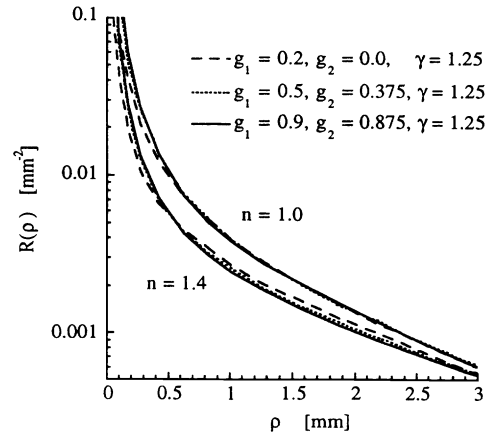
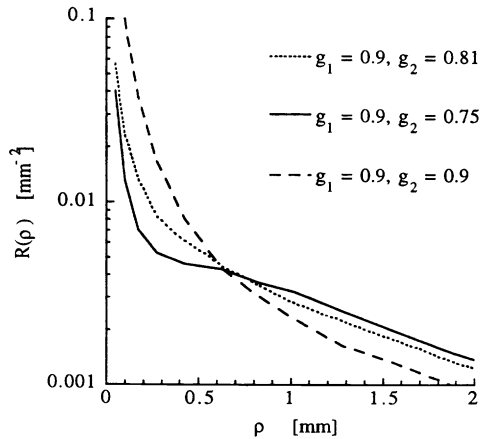


Fig.2 Effect on the second moment of the phase function g_2 on the reflectance, from Monte Carlo simulations. Case of $\mu_s = 1 \text{ mm}^{-1}$ and mismatched boundary condition $n=1.4$. Fig.3 Second order similarity relation $\gamma=(1-g_2)/(1-g_1)$. (Monte Carlo simulations).

3.2. Inverse problem

Our goal is to solve the inverse problem, which consists in extracting optical coefficients from the reflectance data. The measurements of the reflectance intensity $R(\rho)$ and the slope of $\ln R(\rho)$ ($=\partial_\rho \ln R(\rho)$), determined at a single distance can be used to derive μ_s' and μ_a for a given γ value, as already shown in Ref.19. If the γ is correct, the experimental reflectance $R(\rho)$ must fit with a simulation over a large range of distance ρ . Therefore, we defined the following iterative procedure:

- (1) determination of μ_s' and μ_a from $R(\rho=1 \text{ mm})$ and $|\partial_\rho \ln R(\rho=1 \text{ mm})|$ using different γ values (for example $\gamma = 1.0, 1.5, 1.75, 1.9, 2.2$)
- (2) simulations of $R(\rho)$ using the different sets of μ_s' and μ_a obtained from step (1), corresponding to the different γ values.
- (3) comparison between the simulations and the reflectance profile for distances $0.35 < \rho < 1.4 \text{ mm}$.

This last step allows us to determine the value of γ which gives the best fit, and thus select the correct μ_s' and μ_a values. This Steps 1 to 3 can be done iteratively to evaluate γ more precisely. The precision that can be obtained depends on the optical coefficients themselves, and on the experimental uncertainties.

Two important technical points should be noted here. For μ_s' near to 1 mm^{-1} , the determination of μ_s' is only weakly influenced by γ . The differences induced by $\gamma = 1.5$ or $\gamma = 1.9$ on μ_s' are typically 10%. In contrast, absolute determination of μ_a is critically sensitive to γ . However, if γ remains constant, relative variations of μ_a can be still relatively precisely evaluated. A precision of $\pm 0.005 \text{ mm}^{-1}$ was achieved in measurements on Intralipid with various concentrations of dye¹³.

Fig.4 shows an experimental measurement on the human grey matter, plotted with simulation data. It illustrates that adapting the γ value is necessary to fit well the reflectance curve. As already mentioned, an incorrect value of γ will dramatically affect the absolute μ_a value, but only weakly the μ_s' value. The inverse procedure described here is

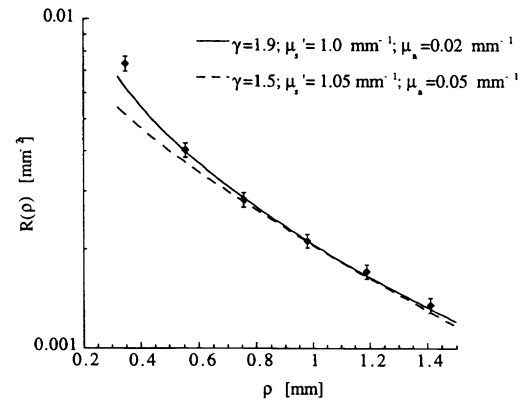


Fig. 4. Effect of the phase function parameter γ on the reflectance. The dots are *in vivo* measurements on human cortex. The solid and broken lines are obtained from Monte Carlo simulations.

currently being optimized, and the accuracy and precision achievable on the determination of μ_a , μ_s' and γ remains under study.

3.3. *In vivo* measurements on brain tissues

Clinical measurements of normal and malignant neural tissues were recorded *in vivo* during brain surgery²⁰. One case (3 year old male) is reported here. Different types of tissues were investigated. Measurements were performed on normal cerebral cortex (temporal lobe) and an optic nerve astrocytoma (size=1.3 cm). Tumor dimensions were estimated from conventional imaging techniques (i.e. Computed Tomography and/or Magnetic Resonance Imaging). Several measurements (typically 6) were performed successively at each location. The intensity fluctuations (typically on the order of 10%) for these measurements were mainly due to tissue heterogeneity and slight probe movements. The average reflectance was calculated for each location, as well as the standard deviation. Note that the uncertainty due to the apparatus, estimated from measurements on a phantom, are much lower (< 5%). Before each set of measurements, the blood from the surgical site was carefully irrigated away with saline, and the probe cleaned with a saline damped sponge. As discussed elsewhere¹⁹, the depth probed is less than about 3 mm. For each tissue type investigated, the influence of surrounding tissues on the measurement is weak. In particular, only gray matter is investigated during the cerebral cortical surface measurements, due to its laminar organization.

The results are reported in Fig 5 and 6. We discussed first the probe measurements. The overall absorption is much higher in the tumor than the cortex presumably due to a greater hemoglobin concentration. Tumors generally induce the formation of vessels and thus should have a higher blood volume fraction. The μ_s' of the tumor is similar to the cortex at $\lambda = 956$ nm. However the variation of μ_s' between $\lambda = 674$ nm and $\lambda = 956$ nm is larger for the tumor than for the cortex: $\mu_s'(\lambda=956 \text{ nm}) - \mu_s'(\lambda=674 \text{ nm}) = 0.57 \text{ mm}^{-1}$ for tumor, $\mu_s'(\lambda=956 \text{ nm}) - \mu_s'(\lambda=674 \text{ nm}) = 0.10 \text{ mm}^{-1}$ for the cortex. Such spectroscopic variations may be attributable to structural differences between tissue types. Indeed such differences may depend on the average size or size distribution of scattering structures within or between cells. The absorption coefficients at $\lambda = 811$ and 849 nm are lower than those obtained at $\lambda = 674$ nm or $\lambda = 956$ nm. This result is consistent with the fact that the main near-infrared tissue chromophores, hemoglobin and water, have absorption maximum at approximately at $\lambda < 700$ nm and $\lambda = 970$ nm, respectively²¹.

The optical coefficients we obtained can be compared to the measurements performed simultaneously with the FDPM technique. One should keep in mind that the depth investigated by FDPM technique is larger compared to the spatially-resolved technique described here. Therefore, differences of optical property values are expected between these two techniques. Interestingly, the decrease of μ_s' from $\lambda = 674$ to 956 nm, is more pronounced in the FDPM data for the cortex, but is very similar for the astrocytoma. Generally the μ_s' values are on the same order between the two methods. The μ_a values are also very close for the cortex measurements. In contrast, for the tumor values (astrocytoma), important differences are found for μ_a between the spatially resolved and FDPM probes. Particularly, the μ_a values obtained by the spatially-resolved probe are significantly larger. This can be explained by the sensitivity of the spatially-resolved probe to the high local hemoglobin content which can be resolved only by the small source-detector separations. In contrast, the large source detector separation employed by the FDPM probe interrogates much greater larger tissue volumes and hence measures average optical properties from multiple structures (e.g. normal and malignant). This also explains why the spatially-resolved probe seems able to distinguish the two tissues (cortex and astrocytoma), whereas much smaller differences are found in the FDPM data

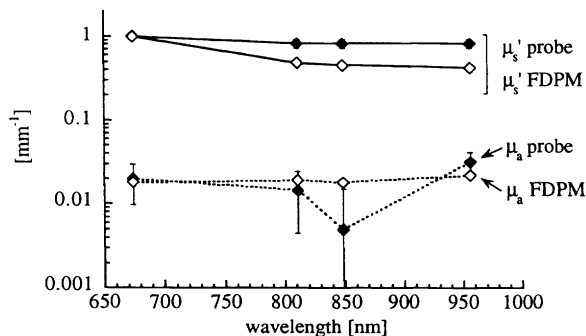


Fig.5 *In vivo* measurements in human cortex.

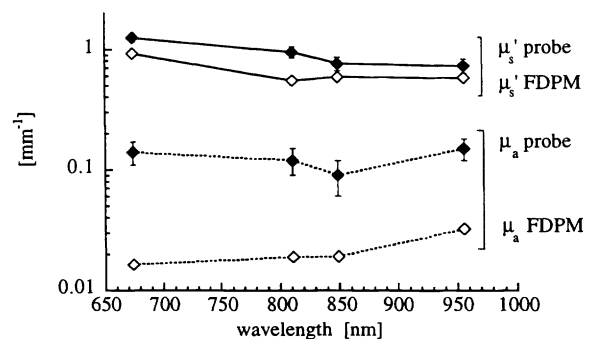


Fig.6. *In vivo* measurements on an astrocytoma of the optic nerve.

4. CONCLUSION

The purpose of this work was to assess the performance of spatially-resolved diffuse reflectance using short source-detector separations (< 1.4 mm). Monte Carlo simulations were used to establish the correspondence between the measured reflectance and the optical properties.

Optical properties determined by this technique are the absorption coefficient μ_a , the reduced scattering coefficient μ_s' , and a parameter of the phase function $\gamma=(1-g_2)/(1-g_1)$, where $g_1(=g)$ and g_2 are the first and second moment of the phase function. Good correlation has been found between spatially-resolved reflectance and simultaneous measurements performed by frequency domain photon migration (FDPM). These two techniques offer interesting complementary features. The spatially resolved probe can potentially provide better differentiation between different types of tissue, due to its sensitivity to local structure. This is due to the fact that substantially smaller volume of tissue is probed. On the other hand, due to physical limitations imposed by large NIR mean absorption lengths in tissue, the precision for μ_a estimate is likely to be worse. Consequently, the short distance, spatially-resolved technique appears to be well suited for clinical settings, that require rapid localized tissue identification, such as endoscopic or needle-based "optical biopsy" and intraoperative tissue mapping for surgical guidance.

ACKNOWLEDGEMENTS

We would like to thank Joshua B. Fishkin, Tuan H. Pham for their help in the FDPM measurements and data processing. We would like to thank also P. Fankhauser for his help in the design of the probe. We acknowledge the Microengineering Department, Swiss Federal Institute of Technology-Lausanne for the Visiting Faculty Fellowship Program. This work was supported by the Swiss National Science Foundation (N0 2053-049628.96), National Institutes of Health (NIH) Laser Microbeam and Medical Program (LAMMP) and Optical Biology facilities (grants, RR-01192 and CA-62203, respectively); NIH grant GM-50958, and DOE grant DE-FG03-91ER61227.

REFERENCES

1. J.B. Fishkin, O. Coquoz, E.R. Anderson, M. Brenner, and B.J. Tromberg, "Frequency-domain photon migration measurements of normal and malignant tissue optical properties in human subject," *Appl. Opt.* 36, 10-20 (1997).
2. B.J. Tromberg, O. Coquoz, J.B. Fishkin, T. Pham, E.R. Anderson, J. Butler, M. Cahn, J.D. Gross, V. Venugopalan, and D. Pham, "Non-invasive measurements of breast tissue optical properties using frequency-domain photon migration," *Phil.Trans.R.Soc.Lond. B.* 352, 661-668 (1997).
3. J.R. Mourant, I.J. Bigio, J. Boyer, R.L. Conn, T. Johnson, and T. Shimada, "Spectroscopic Diagnosis of Bladder-Cancer with Elastic Light-Scattering," *Lasers Surg. Med.* 17, 350-357 (1995).
4. W.-F. Cheong, S.A. Prahl, and A.J. Welch, "A Review of the Optical Properties of Biological Tissues," *IEEE J. Quantum Electron.* 26, 2166-2185 (1990).
5. T. J. Farrell, M. S. Patterson and B. C. Wilson, "A diffusion theory model of spatially resolved, steady -state diffuse reflectance for the non invasive determination of tissue optical properties in vivo," *Med.Phys.* 19, 879-888 (1992).
6. R. Bays, G. Wagnières, D. Robert, D. Braichotte, J.-F. Savary, P. Monnier and H. van den Bergh, "Clinical determination of tissue optical properties by endoscopic spatially resolved reflectometry," *Appl.Opt.* 35 (10), 1756-1766 (1996).
7. A. Kienle, L. Lilge, M.S. Patterson, R. Hibst, R. Steiner, and B.C. Wilson, "Spatially resolved absolute diffuse reflectance measurements for noninvasive determination of the optical scattering and absorption coefficients of biological tissue.," *Appl.Opt.* 35, 2304-2314 (1996).
8. J.S. Fantini, M.A. Franceschini, J.B. Fishkin, B. Barbieri, and E. Gratton, "Quantitative determination of the absorption spectra of chromophores in strongly scattering media: a light-emitting based techniques," *Appl.Opt.* 33, 5204-5213 (1994).
9. L. Reynolds, C. Johnson, and A. Ishimaru, "Diffuse reflectance from a finite blood medium: application to the modeling of fiber optic catheter," *Appl.Opt.* 15, 2059-2067 (1976).
10. K. Ono, M. Kanda, J. Hiramoto, K. Yotsuya, and N. Sato, "Fiber optic reflectance spectrophotometry system for in vivo tissue diagnosis," *Appl. Opt.* 30, 98-105 (1991).
11. J.R. Mourant, I.J. Bigio, D.A. Jack, T.M. Johnson, and H.D. Miller, "Measuring absorption coefficients in small volumes of highly scattering media: source detector separations for which path lengths do not depend on scattering properties," *Appl. Opt.* 36, 5655-5661 (1997).

12. F.P. Bolin, L.E. Preuss, R.C. Taylor and J. Ference, "Refractive index of some mammalian tissues using a fiber optic cladding method," *Appl. Opt.* 28, 2297-2296 (1989).
13. F. Bevilacqua, "Optical characterization of biological tissues in vitro and in vivo", PhD dissertation N° 1781, Swiss Federal Institute of Technology Lausanne (1998).
14. D.R. Wyman, M.S. Patterson, and B.C. Wilson, "Similarity Relations for anisotropic Scattering in Monte Carlo Simulations of Deeply Penetrating Neutral Particles," *J. of Comput.Phys.* 81, 137-150 (1989).
15. P. Marquet, F. Bevilacqua, C. Depeursinge, and E. B. de Haller, "Determination of reduced scattering and absorption coefficients by a single charge-coupled-device array measurement, part I: comparison between experiments and simulations," *Opt.Eng.* 34, 2055-2063 (1995).
16. F. Bevilacqua, P. Marquet, C. Depeursinge, and E. B. de Haller, "Determination of reduced scattering and absorption coefficients by a single charge-coupled-device array measurement, part II: measurements on biological tissues," *Opt.Eng.* 34, 2064-2069 (1995).
17. R.C. Haskell, L.O. Svaasand, T.-T. Tsay, T.-C. Feng, M.S. McAdams, and B.J. Tromberg, "Boundary conditions for the diffusion equation in radiative transfer," *J.Opt.Soc.Am.A.* 11, 2727-2741 (1994).
18. O. Coquoz, J.B. Fishkin and B.J. Tromberg, "MONARCH: Software designed to extract optical properties (absorption, scattering, refractive index) from Frequency-Domain Photon Migration (FDPM) data" Copyright pending, (1997).
19. F. Bevilacqua, D. Piguet, P. Marquet, J. D. Gross, B. J. Tromberg, and C. Depeursinge, "In vivo local optical determination of tissue optical properties," *Proc. SPIE*, Vol. 3194, 262-268 (1998).
20. Protocol and informed consent was obtained for the patient undergoing neurological surgery for an intra-axial brain tumor as demonstrated on conventional neuroimaging. The protocol and informed consent documents were approved by the UCI review board (HS#96-495).
21. M Cope, "The development of a near infrared spectroscopy system and its application for non invasive monitoring of cerebral blood and tissue oxygenation in the newborn infant," Ph.D. Dissertation, University College London, 1991.